Simulation of the Scattering of an Electromagnetic Wave Using Multi-trace Boundary Integral Equations

Simulatie van de Verstrooiing van een Elektromagnetische Golf met behulp van Multi-trace Randintegraalvergelijkingen

by

Annerieke Ohm

to obtain the degree of Bachelor of Science
in Applied Mathematics
at the Delft University of Technology,

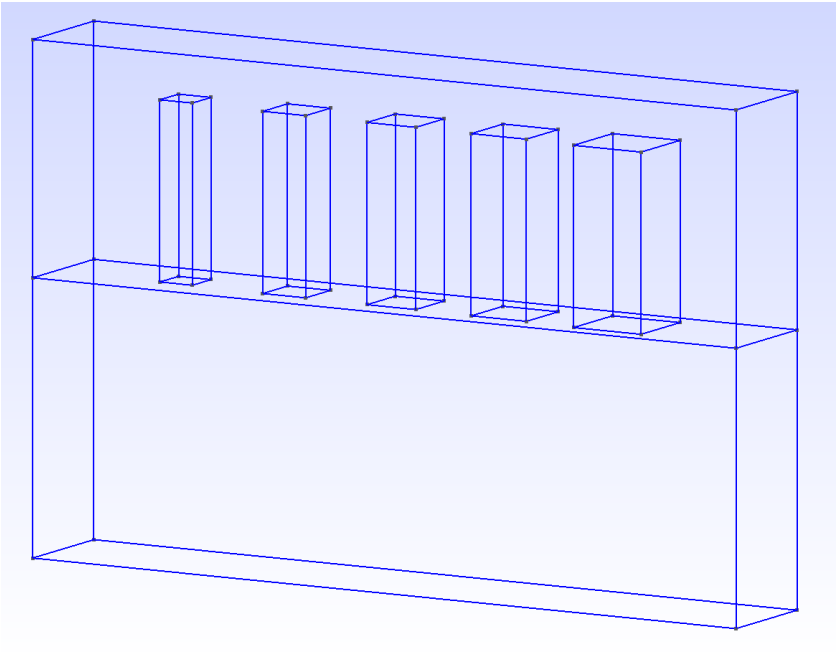

Student number: 4852990
Date: June 29, 2021
Thesis committee: Dr. K. Cools, TU Delft, supervisor
Dr. J. Sauer, TU Delft

TU Delft

Layman's Summary

Metalenz is a spin-off company of Harvard University that works on finding newer and better designs for lenses. To prevent manufacturing designs that might not work, they first want to run computer simulations on their designs. This research focuses on a possible method for these simulations using a test case as design. It turns out that the simulations work, but that they are slow. Therefore, a technique to make the simulations faster is researched. This technique manages to change simulations that take a week to finish into simulations that take a couple of hours to finish. Before Metalenz can start using the simulation techniques, they should be tested for more complicated cases, to make sure they still work when more factors are at play.

Summary

Technology has developed incredibly fast over the last years, so it should come as no surprise that better lenses are being developed as well. One of the companies that focuses on developing lenses is Metalenz, a spin-off company of Harvard University. To prevent having to manufacture lenses that might not work, they want to be able to simulate the scattering of an electromagnetic wave by those designs.

This research focuses on a possible technique for these simulations, using a test case provided by Metalenz as lens design. The test case consists of five pillars, varying in diameter from 132 nm to 274 nm, placed at intervals of 430 nm on a substrate and covered by an encapsulant. The substrate, pillars and encapsulant are all made of a different material. Existing techniques are able to simulate the scattering at the points where the wave moves from one material to another. However, problems occur at points where three or more materials meet. Therefore, a relatively new technique called the multi-trace method is used. The idea of the multi-trace method, is to put a tiny layer of background material, in this case air, between any two surfaces. In this way, there are no points where three or more materials meet, meaning the existing techniques can be used to simulate the scattering further.

This research treats three different scenarios for simulation. First, it simulates the situation where there is just one pillar placed on a substrate and covered with an encapsulant to see whether the programme written gives the expected results. It turns out that the programme works and the simulations give valid results. However, the program also needs a large amount of memory to be able to run. All simulations in this project were run on a standard laptop, meaning that the amount of memory available was limited and running a simulation for all five pillars at once, probably was not possible.

However, it was important to determine whether having multiple pillars affected the working of the multi-trace method and the program. Therefore, the choice was made to run a simulation for two pillars placed 430 nm apart on a substrate and covered with an encapsulant. By adding a second pillar, the total surface area increases, which leads to more unknowns. Consequently, the simulation for two pillars is less precise than for one pillar. However, it is precise enough to be able to conclude that the simulation still works and there is reason to believe it will also work with more pillars.

The third scenario tries to decrease the amount of time and memory required to run the simulations. The part of the simulation that takes up most time and memory is an iterative process to solve a matrix equation of the form $Ax = b$. To decrease the amount of time and memory required, the number of iterations should be decreased. One way to do this is to multiply both sides of the equation with some preconditioner matrix P, where P is close to A^{-1}. Two possible preconditioners are tested, the Calderón preconditioner and the block-Jacobi preconditioner. The Calderón preconditioner needs four times less iterations than the original number of iterations. The block-Jacobi needs about 85 times less iterations than the original number of iterations.

This research shows that it is possible to use the multi-trace method to simulate the scattering of an electromagnetic wave by both one and two pillars. The results also give reason to believe the multi-trace method will work when there are more than two pillars. However, to run those simulations it is advised to use a preconditioner. The block-Jacobi preconditioner seems like a good option to decrease the amount of time and memory required by the program, although it is recommended to run several other simulations with a different number of unknowns to check. If it turns out that these techniques still work for those situations, they should be tested for complicated objects. For example, when the five pillars are not all made of the same material, or there are 25 pillars located in a five by five square. However, to do this it is recommended to use a better computer, or maybe even a supercomputer, like the one TU Delft is planning to build.

Contents

1

Introduction and Problem Statement

All around the world people have been working from home for over a year, making digitisation more important than ever. Seeing other people mostly happens via pictures and video-calls. Can you imagine living the last year without cameras or webcams? This is just one of many uses of lenses nowadays. Technology has developed incredibly fast over the last years, so it should come as no surprise that better lenses are being developed as well. One of the companies that focuses on developing lenses is Metalenz. Metalenz is a spin-off company of Harvard University and they "design, manufacture and sell meta-optics into high volume applications including consumer electronics, mobile phone, and automotive."[8]. To be able to design a better lens, it is important to predict whether a possible design could work. This prevents them from having to manufacture every possible design, many of which might not work. By first running a simulation, Metalenz can predict whether a design is worth manufacturing and in this way they can reduce the costs. However, while there exist working simulation techniques for lenses consisting of one material, these do not necessarily work for lenses made of several materials. Luckily, there is an upcoming technique called "multi-trace". This research will focus on using multi-trace to simulate the scattering of an electromagnetic wave by an example object provided by Metalenz.

The main question Metalenz had was whether the multi-trace method could be used to simulate their lens designs. To do this, they provided a test case. The object in this test case consists of 5 pillars, varying in diameter from 132 nm to 274 nm, placed at intervals of 430 nm on a substrate and covered by an encapsulant. The object is presented in the figure below. The dimensions of the pillars can be found in the table below. The height of the pillars is 650 nm and the height of the encapsulant is 850 nm. The refractive indices of the 3 materials are given by n_encapsulant, n_pillar and n_substrate in the figure, with values of 1.58, 3.70 and 1.46, respectively. Metalenz also provided that the incoming planewave has a wavelength of 940 nm.

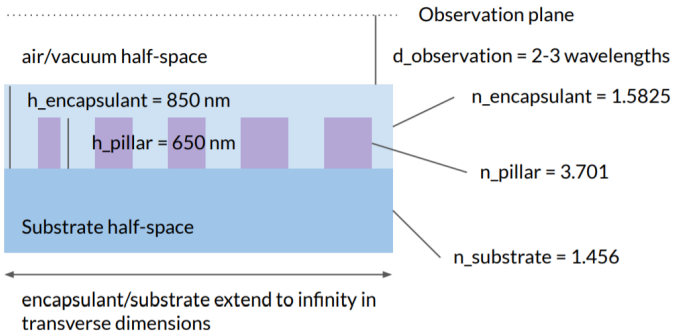

Diagram showing the object of the test case provided by Metalenz.

Pillar	x(nm)	Diameter(nm)
1	-860	132
2	-430	174
3	0	198
4	430	224
5	860	274

Diameter dimensions of the pillars and their spacing on the substrate.

To be able to do these simulations, some background information is needed, this will be presented in chapter 2. Chapter 3 shows the method and results of running a multi-trace simulation on a setup with one pillar. After that, in chapter 4, a simulation is run on a setup with two pillars. Chapter 5 discusses a way to decrease the memory and time required by the programs. Finally chapter 6 tells what can be concluded from this research and what further research is recommended.

This research will only discuss some of the main results. For the programs returning the full results, the reader is referred to [9].

2

Background and State of the Art

This chapter will provide a short overview of the background information needed to do the simulations. Most of this information is retrieved from the PhD of Yves Beghein[1]. Therefore, there is a large overlap between the two. For a more thorough explanation, the reader is referred to textbooks like [6] and [7].

2.1. Maxwell's Equations

Light is an electromagnetic wave. This means that it is a wave created by the interaction between electric and magnetic fields. This interaction can be mathematically described by Maxwell's equations: [1]

$$\nabla \times e(r,t) = -\partial_t b(r,t) \tag{2.1}$$
$$\nabla \times h(r,t) = \partial_t d(r,t) + j(r,t) \tag{2.2}$$
$$\nabla \cdot d(r,t) = \rho(r,t) \tag{2.3}$$
$$\nabla \cdot b(r,t) = 0, \tag{2.4}$$

where $e(r,t)$ represents the electric field at position r and time t; $h(r,t)$ represents the magnetic field; $b(r,t)$ and $d(r,t)$ are the magnetic and electric flux density, respectively; and $j(r,t)$ and $\rho(r,t)$ are the electric currents and electric charges that physically induce these fields. [1]

Equation 2.1 is a form of what is known as Faraday's law, stating that a changing magnetic field, produces an electric current and with that, produces an electric field. Therefore the value of the electric field at a point depends on the rate at which a magnetic field changes at that point. [6]

Equation 2.2 is an adjusted form of Ampère's law. This equation mathematically represents the phenomenon of an electric current generating a magnetic field around it. Which means that the value of the magnetic field at a point depends on the electric current and electric charges present at that point. [6]

Equation 2.3 is known as Gauss's Law, stating that the change in the electric field depends on the electric charges and currents present. Gauss's law comes from Coulomb's Law stating that the force between two charged particles depends on the magnitude and type of each charge and the distance between them. Furthermore, it states that the direction of this force is along the line that joins the charges. This is mathematically described by equation 2.3. [6]

Equation 2.4 describes the absence of free magnetic poles, meaning that no matter how small a particle is, it will never have a magnetic charge. This is also known as a magnetic dipole. [6]

These equations can be slightly adjusted to make them symmetrical and with that, make them more convenient for calculations. To do this, two quantities are added: the magnetic current density $m(r,t)$ and the magnetic charge density $\kappa(r,t)$. Adding these quantities is possible because their value is

physically zero, meaning they do not change the value of the calculated fields. Adding these quantities results in the following equations: [1]

$$\nabla \times e(r,t) = -\partial_t b(r,t) - m(r,t) \tag{2.5}$$
$$\nabla \times h(r,t) = \partial_t d(r,t) + j(r,t) \tag{2.6}$$
$$\nabla \cdot d(r,t) = \rho(r,t) \tag{2.7}$$
$$\nabla \cdot b(r,t) = \kappa(r,t). \tag{2.8}$$

2.2. Medium Dependence

Maxwell's equations are true for any material. However, the material does affect the electromagnetic field. Therefore, the medium should be taken into account when modelling electromagnetic fields. This can be done using constitutive equations.[7] The constitutive equations show the relation between the field quantities, $e(r,t)$ and $h(r,t)$, and the flux densities, $d(r,t)$ and $b(r,t)$. The equations are given by:[1]

$$d(r,t) = \epsilon(r,t) * e(r,t) \tag{2.9}$$
$$b(r,t) = \mu(r,t) * h(r,t). \tag{2.10}$$

The material parameters ϵ and μ are time- and place-dependent. However, the materials in the specific application of this thesis are not time-dependent and can be assumed to be piecewise homogeneous. This removes the time- and place-dependency, reducing the equations to:[1]

$$d(r,t) = \epsilon * e(r,t) \tag{2.11}$$
$$b(r,t) = \mu * h(r,t). \tag{2.12}$$

2.3. Boundary Conditions

The Maxwell equations are valid in a continuous medium. At points located on the boundary between two different media, however, the equations cannot be applied.[7] Consider the following situation. Let $\Omega \subset \mathbb{R}^3$. Let its surface be denoted by Γ and let n be the outward pointing normal vector. Let the following be defined for every point $r \in \Gamma$:[1]

$$e^+(r,t) = \lim_{r' \to r} e(r',t) \qquad \text{for } r' \in \mathbb{R}^3 \backslash \Omega \tag{2.13}$$
$$e^-(r,t) = \lim_{r' \to r} e(r',t) \qquad \text{for } r' \in \Omega. \tag{2.14}$$

Define h^+, h^-, d^+, d^-, b^+ and b^- in a similar way. If there is a source located on boundary γ, then the boundary conditions are defined as follows:[1]

$$n \times e^+ - n \times e^- = -m \tag{2.15}$$
$$n \times h^+ - n \times h^- = j \tag{2.16}$$
$$n \cdot d^+ - n \cdot d^- = \rho \tag{2.17}$$
$$n \cdot b^+ - n \cdot b^- = \kappa. \tag{2.18}$$

These boundary conditions describe the behaviour of the field at the discontinuous points in the domain. The Maxwell equations describe the behaviour at all continuous points. Therefore, both are needed to simulate the behaviour throughout the entire domain.[7]

2.4. Boundary Sources

Define Ω, Γ and n as in the previous section. Let $j_\Omega(r,t)$ and $m_\Omega(r,t)$ be the electric and magnetic currents located inside Ω. Furthermore, suppose that the electric and magnetic fields generated by these currents are denoted by $e(r,t)$ and $h(r,t)$, respectively. If we place the following boundary conditions on the boundary of Ω,[1]

$$j_{eq}(r,t) = n \times h(r,t) \qquad r \in \Gamma \tag{2.19}$$
$$m_{eq}(r,t) = -n \times e(r,t) \qquad r \in \Gamma, \tag{2.20}$$

then the following is a solution of both Maxwell's equations 2.5-2.8 as the boundary conditions 2.15 - 2.18:

$$\bar{e}(r,t) = \begin{cases} e(r,t) & r \in \mathbb{R}^3 \backslash \Omega \\ 0 & r \in \Omega \end{cases} \tag{2.21}$$

$$\bar{h}(r,t) = \begin{cases} h(r,t) & r \in \mathbb{R}^3 \backslash \Omega \\ 0 & r \in \Omega. \end{cases} \tag{2.22}$$

This means that sources inside Ω generate an electromagnetic field outside Ω that is identical to the electromagnetic field generated by placing equivalent currents on the boundary. Similarly, sources outside Ω generate an electromagnetic field inside Ω that is identical to the electromagnetic field generated by placing equivalent currents on the boundary. However, in the second situation, the signs of the equivalent currents should be flipped, since the normal vector is pointing towards the sources instead of away from them.[1]

2.5. Electromagnetic Potentials

Suppose Ω is simply connected, then the medium is homogeneous. Let the permittivity and the permeability be denoted by ϵ and μ, respectively. Assume that there are no magnetic charges or currents present inside Ω. Note that if there are, they can be replaced by equivalent sources on the boundary as stated in section 2.4. From equation 2.8 it then follows that there exists a vector potential $a(r,t)$ such that[1]

$$b(r,t) = \nabla \times a(r,t). \tag{2.23}$$

Combining this with equation 2.5 gives[1]

$$\nabla \times (e(r,t) + \partial_t a(r,t)) = 0. \tag{2.24}$$

From this it then follows that there exists a scalar potential $\phi(r,t)$ such that[1]

$$e(r,t) = -\partial_t a(r,t) - \nabla \phi(r,t). \tag{2.25}$$

There is not a unique possibility for these potentials. However, they can be chosen such that they obey the Lorenz gauge condition:[1]

$$\nabla \cdot a(r,t) + \frac{\partial_t}{c^2} \phi(r,t) = 0, \tag{2.26}$$

where c is the speed of light, equal to $\sqrt{\epsilon\mu}$. If the potentials are chosen in this way, they satisfy the following wave equations:[1]

$$\nabla^2 a(r,t) - \frac{\partial_t^2}{c^2} a(r,t) = -\mu j(r,t) \tag{2.27}$$

$$\nabla^2 \phi(r,t) - \frac{\partial_t^2}{c^2} \phi(r,t) = -\frac{1}{\epsilon} \rho(r,t). \tag{2.28}$$

Similarly, when no electric charges or currents are present, equation 2.7 and equation 2.6 can be written as[1]

$$d(r,t) = -\nabla \times f(r,t) \tag{2.29}$$

$$h(r,t) = -\partial_t f(r,t) - \nabla \psi(r,t), \tag{2.30}$$

where $f(r,t)$ and $\psi(r,t)$ are the vector and scalar potential, respectively. These potentials satisfy the following equations:[1]

$$\nabla^2 f(r,t) - \frac{\partial_t^2}{c^2} f(r,t) = -\epsilon m(r,t) \tag{2.31}$$

$$\nabla^2 \psi(r,t) - \frac{\partial_t^2}{c^2} \psi(r,t) = -\frac{1}{\mu} \kappa(r,t) \tag{2.32}$$

$$\nabla \cdot f(r,t) + \frac{\delta_t}{c^2} \psi(r,t) = 0. \tag{2.33}$$

These two situations can be combined to form the following equations describing the complete electromagnetic field:[1]

$$e(r,t) = -\partial_t a(r,t) - \nabla\phi(r,t) - \frac{1}{\epsilon}\nabla \times f(r,t) \tag{2.34}$$

$$h(r,t) = -\partial_t f(r,t) - \nabla\psi(r,t) + \frac{1}{\mu}\nabla \times a(r,t). \tag{2.35}$$

2.6. Green's Function

To find an explicit formula for the potentials, the following equation should be considered:[1]

$$\nabla^2 G(r,t) - \frac{\partial_t^2}{c^2} G(r,t) = -\delta(r)\delta(t). \tag{2.36}$$

This equation is similar to the equations for the potentials. However, for equation 2.36, the solution in an infinite domain $\Omega = \mathbb{R}^3$ is known. This solution is given by Green's function[1]

$$G(r,t) = \frac{\delta(t - |r|/c)}{4\pi|r|}. \tag{2.37}$$

Green's function represents a spherical wave. Mathematically this wave can be either incoming towards $r = 0$ at $t = 0$ or outgoing from $r = 0$ at $t = 0$. The incoming wave is anti-causal, meaning it does not represent a field generated by a point source. Therefore, the correct solution for this problem is the outgoing spherical wave.[1]

Using equation 2.37, the potentials can be written as follows:[1]

$$a(r,t) = \mu \int_{\mathbb{R}^3} dV' \int_{\mathbb{R}} dt'\, G(r-r', t-t')\, j(r',t') \tag{2.38}$$

$$\phi(r,t) = \frac{1}{\epsilon} \int_{\mathbb{R}^3} dV' \int_{\mathbb{R}} dt'\, G(r-r', t-t')\, \rho(r',t') \tag{2.39}$$

$$f(r,t) = \epsilon \int_{\mathbb{R}^3} dV' \int_{\mathbb{R}} dt'\, G(r-r', t-t')\, m(r',t') \tag{2.40}$$

$$\psi(r,t) = \frac{1}{\mu} \int_{\mathbb{R}^3} dV' \int_{\mathbb{R}} dt'\, G(r-r', t-t')\, \kappa(r',t'). \tag{2.41}$$

Rewriting this gives:

$$a(r,t) = \mu \int_{\mathbb{R}^3} \frac{j(r', t-R/c)}{4\pi R}\, dV' \tag{2.42}$$

$$\phi(r,t) = \frac{1}{\epsilon} \int_{\mathbb{R}^3} \frac{\rho(r', t-R/c)}{4\pi R}\, dV' \tag{2.43}$$

$$f(r,t) = \epsilon \int_{\mathbb{R}^3} \frac{m(r', t-R/c)}{4\pi R}\, dV' \tag{2.44}$$

$$\psi(r,t) = \frac{1}{\mu} \int_{\mathbb{R}^3} \frac{\kappa(r', t-R/c)}{4\pi R}\, dV', \tag{2.45}$$

where $R = |r - r'|$[1].

2.7. Boundary Integral Equations

As mentioned in section 2.4, the electromagnetic field inside a homogeneous domain can be constructed from the surface currents on the boundary of the domain. Consider a domain Ω with boundary Γ in an infinite homogeneous medium. Suppose $j(r,t)$ is an electric current on Γ. Let ϵ and μ be the permittivity and the permeability of the medium, respectively. The electric and magnetic fields generated

by this current are:[1]

$$\begin{aligned} e(r,t) &= -\partial_t a(r,t) - \nabla\phi(r,t) \\ &= -\mu\partial_t \int_\Gamma \frac{j(r',t-R/c)}{4\pi R}\, ds' + \frac{1}{\epsilon}\nabla \int_\Gamma \frac{\int_{-\infty}^{t-R/c} \nabla'\cdot j(r',\tau)\, d\tau}{4\pi R}\, ds' \qquad (2.46) \\ h(r,t) &= \frac{1}{\mu}\nabla\times a(r,t) \\ &= \nabla\times\int_\Gamma \frac{j(r',t-R/c)}{4\pi R}\, ds'. \qquad (2.47) \end{aligned}$$

Let $\eta = \sqrt{\mu/\epsilon}$ denote the characteristic impedance of the medium. Taking the limits of equations 2.46 and 2.47 in a similar way as in equations 2.13 and 2.14 results in the following:[1]

$$n\times e^{\pm}(r,t) = \eta(\mathcal{T}j)(r,t) \qquad (2.48)$$

$$n\times h^{\pm}(r,t) = -(\mathcal{K}j)(r,t) \pm \frac{1}{2}j(r,t), \qquad (2.49)$$

where $\mathcal{T}$, the electric field integral equation (EFIE) operator, and $\mathcal{K}$, the magnetic field integral equation (MFIE) operator, are defined as:[1]

$$\mathcal{T}j(r,t) = \mathcal{T}_s j(r,t) + \mathcal{T}_h j(r,t) \qquad (2.50)$$

$$\mathcal{T}_s j(r,t) = -\frac{1}{c} n\times\int_\Gamma \frac{\partial_t j(r',t-R/c)}{4\pi R}\, ds' \qquad (2.51)$$

$$\mathcal{T}_h j(r,t) = c\, n\times p.v.\int_\Gamma \nabla \frac{\int_0^{t-R/c}\nabla'\cdot j(r',t')\, dt'}{4\pi R}\, ds' \qquad (2.52)$$

$$\mathcal{K}j(r,t) = -n\times p.v.\int_\Gamma \nabla\times\frac{j(r',t-R/c)}{4\pi R}\, ds'. \qquad (2.53)$$

Similarly, if $m(r,t)$ is a magnetic surface current, the following equations can be found:[1]

$$n\times e^{\pm}(r,t) = \mathcal{K}m(r,t) \pm \frac{1}{2}m(r,t) \qquad (2.54)$$

$$n\times h^{\pm} = \frac{1}{\eta}\mathcal{T}m(r,t). \qquad (2.55)$$

Omitting the dependence on r and t, we get the following equation:[1]

$$\begin{pmatrix} -n\times e^{\pm} \\ n\times h^{\pm}\end{pmatrix} = \begin{pmatrix} -\mathcal{K}\pm\frac{1}{2} & -\eta\mathcal{T} \\ \frac{1}{\eta}\mathcal{T} & -\mathcal{K}\pm\frac{1}{2}\end{pmatrix}\begin{pmatrix} m \\ j\end{pmatrix}. \qquad (2.56)$$

2.8. PMCHWT

Suppose Ω is dielectric, meaning that it is an electric insulator, with permittivity and permeability ϵ' and μ'. Let Ω be surrounded by a medium with permittivity and permeability ϵ and μ. Furthermore, suppose that there are no sources inside Ω. Then, outside Ω the fields satisfy the following equation:[1]

$$\begin{pmatrix} -n\times e^{+} \\ n\times h^{+}\end{pmatrix} = \begin{pmatrix} -\mathcal{K}+\frac{1}{2} & -\eta\mathcal{T} \\ \frac{1}{\eta}\mathcal{T} & -\mathcal{K}+\frac{1}{2}\end{pmatrix}\begin{pmatrix} -n\times e^{+} \\ n\times h^{+}\end{pmatrix} + \begin{pmatrix} -n\times e^{i+} \\ n\times h^{i+}\end{pmatrix}, \qquad (2.57)$$

where e^i and h^i are the incident, or incoming fields created by sources outside Ω. The fields inside Ω satisfy the following equation:[1]

$$\begin{pmatrix} -n\times e^{-} \\ n\times h^{-}\end{pmatrix} = \begin{pmatrix} \mathcal{K}'+\frac{1}{2} & \eta'\mathcal{T}' \\ -\frac{1}{\eta'}\mathcal{T}' & \mathcal{K}'+\frac{1}{2}\end{pmatrix}\begin{pmatrix} -n\times e^{+} \\ n\times h^{+}\end{pmatrix}, \qquad (2.58)$$

where ϵ' and μ' define the operators and quantities with a prime and ϵ and μ define the operators and quantities without a prime. [1]

Combining the boundary conditions 2.15 and 2.16 with the assumption that there are no sources on Γ, we find that the equations $n \times e^+ = n \times e^-$ and $n \times h^+ = n \times h^-$ must hold. Application to 2.57 and 2.58 results in the equation known as the Poggio-Miller-Chan-Harrington-Wu-Tsai (PMCHWT) equation:

$$\begin{pmatrix} -n \times e^{i+} \\ n \times h^{i+} \end{pmatrix} = \begin{pmatrix} \mathcal{K} + \mathcal{K}' & \eta\,\mathcal{T} + \eta'\,\mathcal{T}' \\ -\frac{1}{\eta}\mathcal{T} - \frac{1}{\eta'}\mathcal{T}' & \mathcal{K} + \mathcal{K}' \end{pmatrix} \begin{pmatrix} -n \times e^{+} \\ n \times h^{+} \end{pmatrix}. \tag{2.59}$$

2.9. Frequency Domain

The previous equations depend on the time t and place r. However, the simulation is based on a frequency ω and place r. The frequency is known and only a limited number of frequencies need to be considered. Fortunately, the equations can be made frequency- and place-dependent by applying the Fourier transform. The Fourier transform $X(\omega)$ of a quantity $x(t)$ is given by[1]

$$X(\omega) = \mathcal{F}\{x\}(\omega) = \frac{1}{\sqrt{2\pi}} \int_{\mathbb{R}} x(t)\, e^{-j\omega t}\, dt \tag{2.60}$$

$$x(t) = \mathcal{F}^{-1}\{x\}(t) = \frac{1}{\sqrt{2\pi}} \int_{\mathbb{R}} X(\omega)\, e^{j\omega t}\, dt. \tag{2.61}$$

From this it follows that $\mathcal{F}\{\partial_t x\}(\omega) = j\omega X(\omega)$, meaning that the Maxwell equations become[1]

$$\nabla \times E(r) = -j\omega B(r) - M(r) \tag{2.62}$$

$$\nabla \times H(r) = j\omega D(r) + J(r) \tag{2.63}$$

$$\nabla \cdot D(r) = P(r) \tag{2.64}$$

$$\nabla \cdot B(r) = K(r), \tag{2.65}$$

where the dependence om ω is omitted.

To get the frequency domain PMCHWT equation, the same steps can be followed as in the case of the time domain PMCHWT equation, but with the Fourier transforms of the equations. This means that the constitutive equations 2.11 and 2.12 become:[1]

$$D(r) = \epsilon E(r) \tag{2.66}$$

$$B(r) = \mu H(r). \tag{2.67}$$

Substitution into equations 2.62-2.65 gives[1]

$$\nabla \times E(r) = -j\omega\mu H(r) - M(r) \tag{2.68}$$

$$\nabla \times H(r) = j\omega\epsilon D(r) + J(r) \tag{2.69}$$

$$\nabla \cdot D(r) = P(r) \tag{2.70}$$

$$\nabla \cdot B(r) = K(r), \tag{2.71}$$

From this, the electromagnetic potentials and their integral representation can be derived. However, the Green's function is now given by

$$\nabla^2 G(r) + \frac{\omega^2}{c^2} G(r) = -\delta(r) \tag{2.72}$$

$$G(r) = \frac{e^{-jk|r|}}{4\pi|r|}, \tag{2.73}$$

where $k = \omega/c$.

Continuing this way, the following expressions for the boundary integral operators can be found:[1]

$$(\mathcal{T}_k J)(r) = (\mathcal{T}_{s,k} J)(r) + (\mathcal{T}_{h,k} J)(r) \tag{2.74}$$

$$(\mathcal{T}_{s,k} J)(r) = -jkn \times \int_\Gamma \frac{e^{-jkR}}{4\pi R} J(r')ds' \tag{2.75}$$

$$(\mathcal{T}_{h,k} J)(r) = \frac{1}{jk} n \times p.v. \int_\Gamma \nabla \frac{e^{-jkR}}{4\pi R} \nabla' \cdot J(r')ds \tag{2.76}$$

$$(\mathcal{K}_k J)(r) = -n \times p.v. \int_\Gamma \nabla \times \frac{e^{-jkR}}{4\pi R} J(r')ds' \tag{2.77}$$

The frequency domain electric field integral equation, or FD-EFIE, and the frequency domain magnetic field integral equation, or FD-MFIE, are then given by:[1]

$$\eta(\mathcal{T}_k J)(r) = -n \times E^i(r) \tag{2.78}$$

$$(\mathcal{K}_k J)(r) + \frac{1}{2} J(r) = n \times H^i(r), \tag{2.79}$$

which results in the following expression for the frequency domain PMCHWT equation:[1]

$$\begin{pmatrix} -n \times E^{i+} \\ n \times H^{i+} \end{pmatrix} = \begin{pmatrix} \mathcal{K} + \mathcal{K}' & \eta\mathcal{T} + \eta'\mathcal{T}' \\ -\frac{1}{\eta}\mathcal{T} - \frac{1}{\eta'}\mathcal{T}' & \mathcal{K} + \mathcal{K}' \end{pmatrix} \begin{pmatrix} -n \times E^{+} \\ n \times H^{+} \end{pmatrix}. \tag{2.80}$$

2.10. Multi-trace

The technique of the previous paragraphs results in problems at points where 3 or more different materials meet. To solve this, the multi-trace method is used. The idea of the multi-trace method is to put a tiny layer of background material between any two different materials. In this way, there are no points where more than two materials meet and therefore the previous techniques can be used. However, the different domains still influence each other. The result is a matrix consisting of two by two blocks. Each block containing a form of the main matrix of the PMCHWT equation. Where a block located on the diagonal, so in column i and row i, represents the interaction of domain i with itself, so as if there were no other domains. A block located in row i and column j represents the influence of domain j on domain i.[3] For a more thorough explanation of the multi-trace method, see [5] and [2].

2.11. Meshing

In order to apply the multi-trace method, it is important that after separating two domains, that for domain A, each point on the surface that joined the two domains, can be linked to a point on that same surface of domain B and the other way around. To do this, a mesh can be used. A mesh of a surface divides the surface into small shapes, in this case triangles, that cover the entire surface. The smaller the triangles, the finer the mesh and the more precise the calculations are, but also the more complicated they are.[3]

3

Simulation of Scattering by 1 Pillar

This chapter will show how the scattering of an electromagnetic wave by a setup with one pillar can be simulated using Julia. It will first explain what the original problem of Metalenz was and why and how it was reduced to a smaller subproblem. Next, it will explain what method was used to simulate the scattering for this subproblem. Finally, it will discuss what results were found.

3.1. Problem definition

This section first describes the original problem statement given by Metalenz. After that, it will describe what subproblem was solved first.

3.1.1. Original Problem

The main question Metalenz had was whether the multi-trace method could be used to simulate their lens designs. To do this, they provided a test case. The object in this test case consists of five pillars, varying in diameter from 132 nm to 274 nm, placed at intervals of 430 nm on a substrate and covered by an encapsulant. The object is presented in figure 3.1 and the dimensions of the pillars can be found in table 3.1 The height of the pillars is 650 nm and the height of the encapsulant is 850 nm. The refractive indices of the three materials are given by n_encapsulant, n_pillar and n_substrate in figure 3.1, with values of 1.58, 3.70 and 1.46, respectively. Metalenz also provided that the incoming planewave has a wavelength of 940 nm.

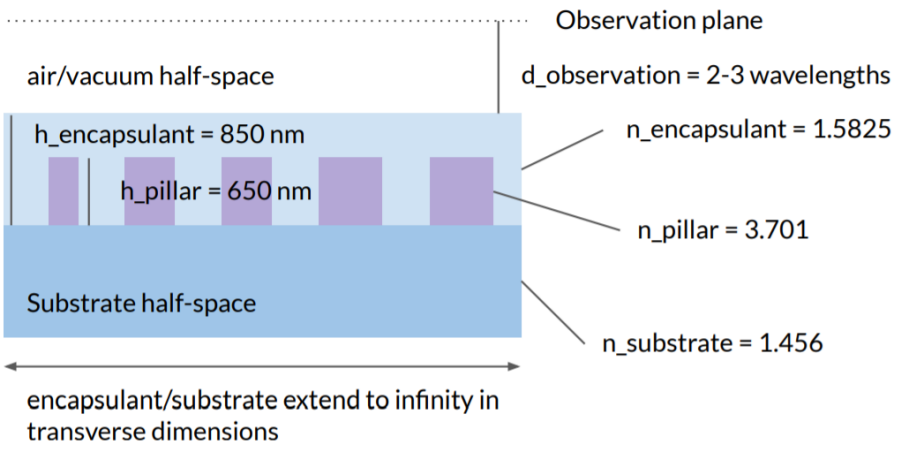

Figure 3.1: Diagram showing the object of the test case provided by Metalenz.

Pillar	x(nm)	Diameter(nm)
1	-860	132
2	-430	174
3	0	198
4	430	224
5	860	274

Table 3.1: Diameter dimensions of the pillars and their spacing on the substrate.

3.1.2. Subproblem

This chapter focuses on a subproblem of the test case. Before simulating for all five pillars at once, it is useful to know whether the program works and whether the results produced are plausible. Therefore, the test case was divided into five smaller test cases, all containing one of the five pillars on a substrate and covered by an encapsulant.

3.2. Method

This section describes the method used to find a solution for the problem. It will first explain how multi-trace works for this object. After that, it will explain how the program Gmsh was used to create a 3D-representation and mesh of the lens made with one cylinder. Next, it will explain the initial program received. Finally, it will explain how this program was adjusted to fit the specific problem.

3.2.1. Multi-trace

To simulate the scattering of the electromagnetic field by one pillar, the multi-trace method is used. This means that between any two materials, a thin layer of the background material is added. In this case, the object consists of three different materials; the pillar, the substrate and the encapsulant. Therefore, these three parts are moved slightly apart and a layer of background material, in this case air, is added in between. This is visually demonstrated in figure 3.2.

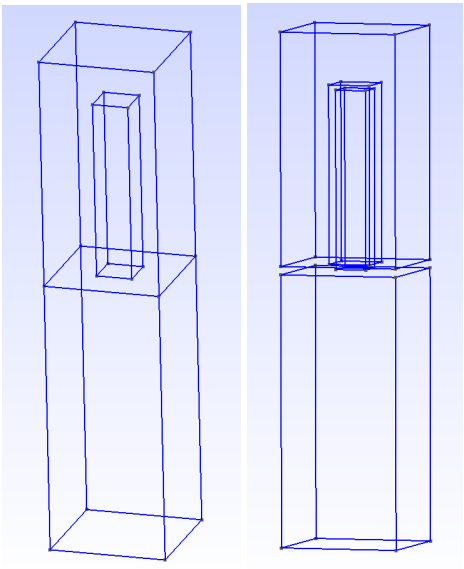

Figure 3.2: Left: The setup of 1 pillar on the substrate covered with the encapsulant. Right: Visual representation of the multi-trace method. A thin layer of air is added between every two materials.

This setup has four different materials, each part of the object is a different material and the background medium is the fourth. Metalenz provided the refraction indices and the wavelength, but the program uses the wavenumber k and and characteristic impedance η, so these have to be calculated from the given information. The background medium is air, meaning that the wavenumber is given by the frequency of the wave Ω, which, by definition, is given by $\Omega = \frac{2\pi}{\lambda}$, where λ is the wavelength. For

any other medium, the wavenumber k_i of another medium is given by $k_i = n_i \cdot k_0$, where k_0 is the wavenumber of air. The characteristic impedance is given by $\eta = \sqrt{\mu/\epsilon}$ and the refraction index is given by $n = \mu \cdot \epsilon$. However, since neither μ nor ϵ is known, η cannot be calculated from n directly. One option is to assume that μ is in vacuum, because then μ is a known constant and therefore η can be calculated. Another option is to assume η is constant. In this case, the second option was chosen and η was assumed to be equal to 1.[3]

3.2.2. Gmsh

Gmsh is a program that allows one to create a 1D, 2D and 3D mesh of an object. For information on the workings of Gmsh, the reader is referred to their official website [4].

For the multi-trace method it is important that every triangle of the mesh of one surface can be linked to a triangle of the other surface at the part where they were connected. To do this, the object is meshed before the different materials are separated. In Gmsh this is possible by defining so-called ”physical groups”. In this case we have physical groups forming surfaces, meaning that a physical group is a set of surfaces, forming one larger surface. For example, to form the surface of the pillar, all six sides of the pillar are added to the same physical group. One surface can be added to more than one physical group. This allows us to add the surface where two materials meet, to both physical groups. Since it is the exact same surface, the mesh of the surface is the same. So every triangle on the surface of one material can be linked to a triangle on the surface of the other material. The size of these triangles is determined by a variable h, where a smaller h means smaller triangles, making the mesh, and therefore our simulation, more precise. The mesh of this setup can be found in figure 3.3. After meshing, Gmsh allows calling these physical groups separately into the Julia program. The next subsection will explain how this Julia program applies the multi-trace method to these physical groups.

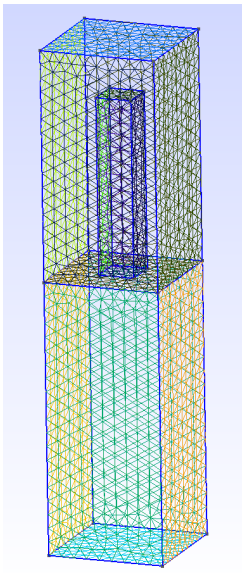

Figure 3.3: The mesh of the setup with 1 pillar, created in Gmsh.

3.2.3. Original Program

At the start of this project an example program was provided by Dr. K. Cools. This program was used as the basis for all simulations in this project. The full program can be found at [9]. The example program simulates the scattering of an incident electromagnetic field by 2 boxes and a thin sheet, where one box and the sheet are perfect electric conductors and the other box is penetrable.

In order to understand how the program should be adjusted to be used for the problem of Metalenz, it is important to first understand how the program works. First, the setup is loaded from Gmsh. In this case, none of the surfaces were added to two physical groups, so the boxes are added together in

lines 42-43. As mentioned in section 2.10, the multi-trace method assumes that all normal vectors are pointed outwards. This is not necessarily the case in Gmsh, therefore, lines 37-49 are used to orient all the surfaces in such a way that the normal vectors are pointed outwards. Lines 51-62 contain the material parameters. After that, the incident field is defined and the basis functions are created. Lines 81-89 define the setup of the PMCHWT equation. After which the matrix A and the vector b from the matrix equation $Ax = b$ are formed by assemblesys and assemblerhs, respectively. Line 93 calculates vector x by iterating over possible solutions. This x is the solution to the problem.

The remainder of the program focuses on visualising this solution. In lines 102-107, the calculated electric and magnetic currents are selected. Lines 123-140 then calculate the electromagnetic field based on these currents. After this, the fields are plotted in a heatmap.

3.2.4. Program Adjustments

The difference between the example problem and the subproblem with one pillar is the object simulated on. However, to change this in the program is takes more than just changing the object loaded from Gmsh. The full programs for the five single pillars can be found at [9]. The main changes in the program will be explained briefly.

First, the physical groups that make up the object are loaded from Gmsh. The boxes do not have to be added together anymore, because surfaces were added to several physical groups, meaning that all three parts are complete. After that, the material parameters are adjusted to be different for all four materials. The next change is in the matrix. The matrix is adjusted to be correct for the PMCHWT-equation for this setup. This matrix is built up of two by two blocks, where every block describes the interaction between two of the three physical groups. The two by two blocks on the diagonal of the matrix describe the interaction of a physical group with itself. Furthermore, the range in lines 120-122 is adjusted to make sure it intersects the pillar. Finally, two extra lines were added to calculate the fields based on the currents, because by having three blocks instead of two blocks and a slab, there are two extra boundary currents.

3.3. Results

This section shows the results found by running the program with the adjustments. It also shows how the results can be used to determine whether the solution is valid.

After running the program, the results are visualised via heat maps. These heat maps show the value of the electric or magnetic field at all points within the range set in lines 120-122. They can be used to determine whether the solution is valid, meaning it is indeed a solution to the Maxwell equations.

We will begin with the electric field of the pillar with smallest diameter, pillar 1. To determine whether the solution is valid, several aspects have to be checked. First, the tangential component of the complete electric field, shown in figure 3.4, must be continuous[7][3]. For figure 3.4 this means that for any vertical line, the field should be continuous from the bottom to the top. It can be seen that this is indeed the case. There are a couple of points on the boundary where the field seems to be discontinuous, but this can be attributed to numerical errors.

Furthermore, the inward pointing electric field, should only exist inside the object, outside it should be equal to zero. This should also hold for every part of the object separately.[3] Figure 3.5 shows the inward pointing components of the electric field of pillar 1. It can be seen that this requirement is met, all four heat maps have a field that only exists inside the object and is equal to zero outside the object.

The third requirement is that the outward pointing electric field component of the total object only exists outside the object. For the separate parts of the object this does not have to hold, because the other parts also contain part of the boundary, meaning that the field can be reflected into each part. Figure 3.6 shows the outward pointing electric field components. It can be seen that this requirement is also met. For the total outward pointing electric field, the field only exists outside the object and is equal to zero inside the object. For the separate parts, this is not the case, but it does not have to be, so the

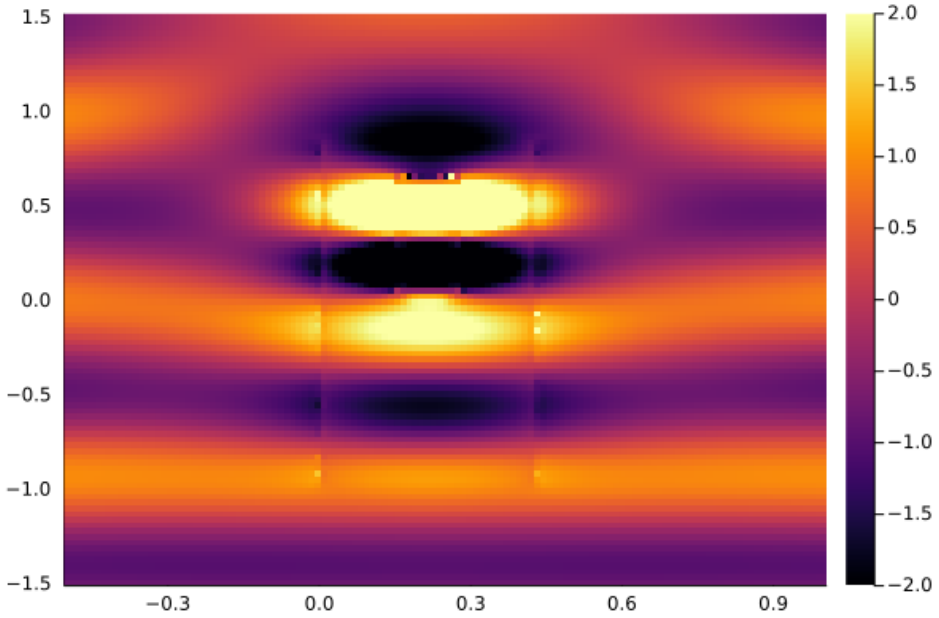

Figure 3.4: Heat map showing the x-component against the z-component of the total electric field of pillar 1. To be a solution to the Maxwell equations, the map should be continuous when walking from the bottom to the top.

requirement is still met.

Finally, this should also hold for the magnetic field of this pillar. The inward and outward pointing components are very similar and can be found by running the program called “Pillar1_132nm.jl” from [9]. The total magnetic field can be found in figure 3.7. The continuity requirement of the tangential component means that the magnetic field should be continuous when walking over a horizontal line from left to right through the heat map. It can be seen that this is indeed the case. There are a couple of points on the boundary where the field seems to be discontinuous, but this can be attributed to numerical errors.

For this project the values of the electromagnetic fields are not important. It only focuses on whether or not the scattering can be simulated and whether this simulation gives a valid solution. In that context, the simulations of the other four pillars are very similar. Looking at the heat maps, one can see that the solutions found in these simulations also meet all before-mentioned requirements. The programs to run these simulations can be found at [9].

3.4. Conclusion

The question was whether it is possible to simulate the scattering of an electromagnetic wave by one pillar on a substrate covered with an encapsulant. The solutions to the simulations of the five separate pillars, all meet the requirements to be a solution to the Maxwell equations. Therefore, these solutions do indeed describe an electromagnetic field, meaning that the simulation works. Therefore, we are able to simulate the scattering of an electromagnetic wave by one pillar.

3.5. Discussion

An important point to note is that all simulations were run on a standard laptop. Consequently, there was a limited amount of memory available. Therefore, creating a very fine mesh was not possible, meaning that the simulation is not as accurate as one would like. However, there is no motivation to expect the simulation to not work with a finer mesh.

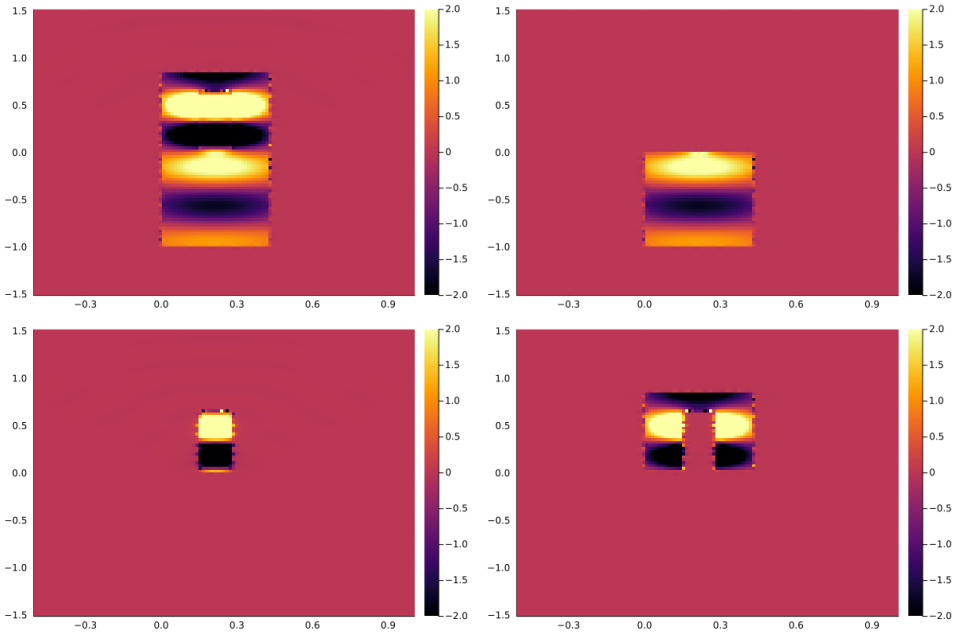

Figure 3.5: The inward pointing electric field components. Top left: The total inward pointing electric field. Top right: the inward pointing electric field component of the substrate. Bottom left: The inward pointing electric field component of pillar 1. Bottom right: The inward pointing electric field component of the encapsulant. In all four cases, the field meets the requirement of only existing inside the object and being equal to zero outside the object.

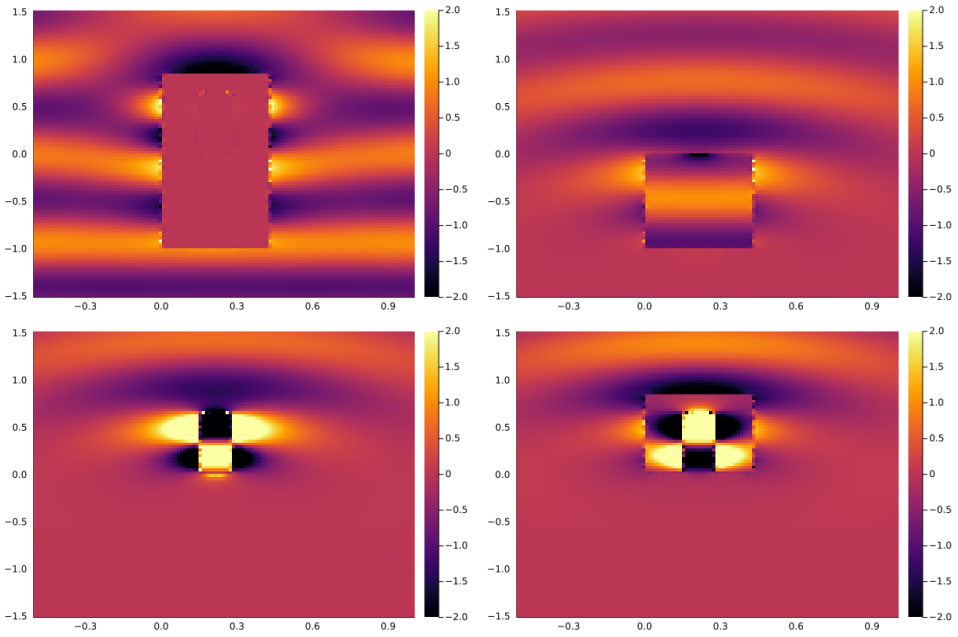

Figure 3.6: The outward pointing electric field components. Top left: the total outward pointing electric field component. Top right: the outward pointing electric field component of the substrate. Bottom left: the outward pointing electric field component of pillar 1. Bottom right: the outward pointing electric field component of the encapsulant.

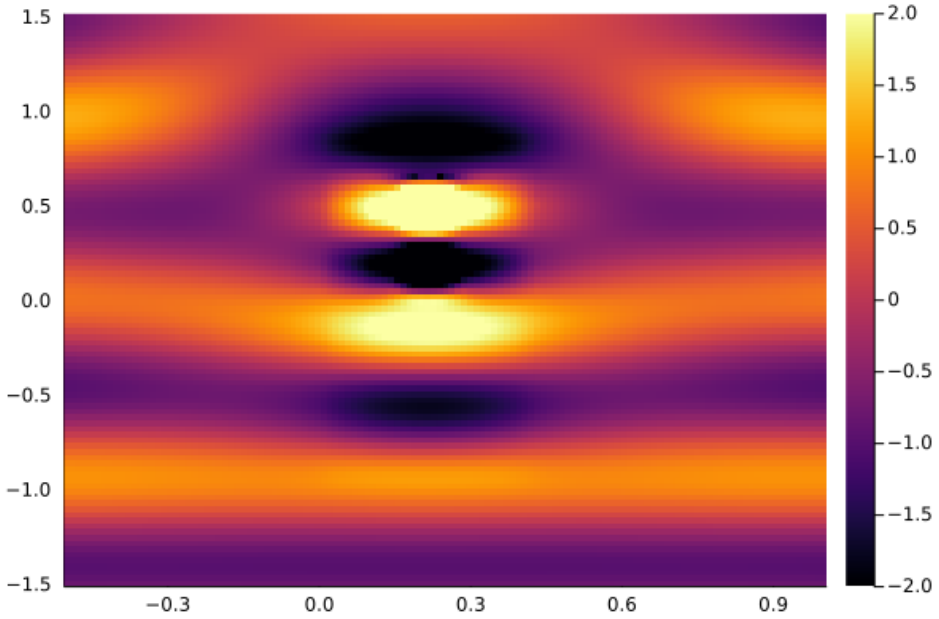

Figure 3.7: Heat map showing the y-component against the z-component of the total magnetic field of pillar 1. To be a solution to the Maxwell equation, the map should be continuous when walking from left to right.

4

Simulation of Scattering by 2 Pillars

The previous chapter showed that simulating the scattering of an electromagnetic field by one pillar on a substrate covered by an encapsulant seems to work for all five different diameters. The next question is whether it also works when there are more pillars on the substrate. This chapter will discuss what happens when there are two pillars on the substrate. It will first explain what the situation looks like, next it will explain how the method and the program change when this second pillar is added. Finally, it will discuss what results are found by running the program.

4.1. Problem Definition

Since all simulations have to be done on a standard laptop, running a simulation on all five pillars together was unfortunately not an option. As mentioned in the previous chapter, the simulation of one pillar already used most of the available memory, preventing the possibility of making the simulation more precise by decreasing h. Therefore, the choice was made to try to simulate a substrate containing two pillars covered by the encapsulant. Only pillars that are located next to each other in the row of all five pillars were simulated. The main question being whether the simulation still works when there are multiple pillars. The reason why this might be more complicated than the case with one pillar, is that the setup now contains two separate domains with the same material parameters. This gives two options in the multi-trace method. They can either be treated as completely separate domains, resulting in two extra rows and columns in the matrix, or they can be treated as one domain, because they have the same material parameters. The second option was chosen, because a bigger matrix would require more memory.

4.2. Method

This section will explain what method was used to find a solution to the problem with two pillars. It will first explain how the multi-trace method works in the case of two pillars. Next it will show how this is implemented with Gmsh. Finally, it will explain what adjustments had to be made to the program.

4.2.1. Multi-trace

To simulate the scattering of the electromagnetic field by two pillars, the multi-trace method is used. This means that between any two materials, a thin layer of the background material is added. In this case, the object consists of three different materials; the two pillars, the substrate and the encapsulant. These four parts are moved slightly apart and a thin layer of air is added between them. This is visually represented in figure 4.1.

4.2.2. Gmsh

The two pillars are made from the same material, this means that they can be treated as one group. The Gmsh representation of this setup therefore still contains three physical groups; the substrate, the pillars and the encapsulant. The mesh of this setup can be found in figure 4.2.

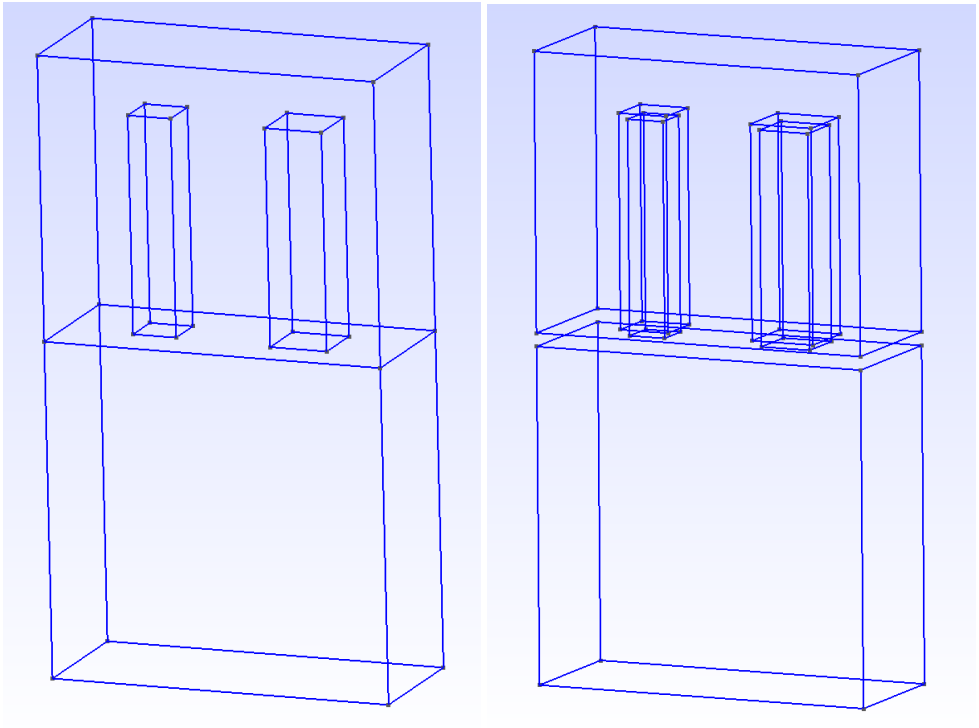

Figure 4.1: Left: The setup of 2 pillars on the substrate covered with the encapsulant. Right: Visual representation of the multi-trace method. A thin layer of air is added between every two materials.

4.2.3. Program Adjustments

The full program can be found at [9]. Since the case for two pillars and the case for one pillar contain the same number of physical groups, the programs are similar as well. Only a couple of small changes had to made. First, there are some small changes in orienting the surfaces, the reason for this is that the way they are oriented after loading them from Gmsh is different, so there is a difference in which orientations have to be changed. The other change is in line 134-136. The object with 2 pillars is wider than the object with 1 pillar. Therefore, the range needs to be adjusted.

4.3. Results

This section discusses the results found by running the program and discusses how to validate these results.

After running the program, the results are visualised via heat maps. These heat maps show the value of the electric or magnetic fields at all points within the range set in lines 134-136. They can be used to determine whether the solution is valid, meaning it is indeed a solution to the Maxwell equations.

Similarly as in section 3.3, the simulations of the different combinations of two neighbouring pillars lead to similar results. Therefore, this section will only discuss the results of the simulation of the two smallest pillars, pillar 1 and pillar 2.

The solution of the simulation of the scattering of an electromagnetic wave by pillar 1 and 2 has to meet the same requirements as the solution of the scattering by one pillar, as discussed in section 3.3.

First, this means that the tangential component of the total electric field, given in figure 4.3, has to be continuous. In the heat map this means that any vertical line has to be a continuous field from the bottom to the top. Figure 4.3 shows that this is indeed the case. There are some points where there seems to be a discontinuity, but that is likely due to numerical errors.

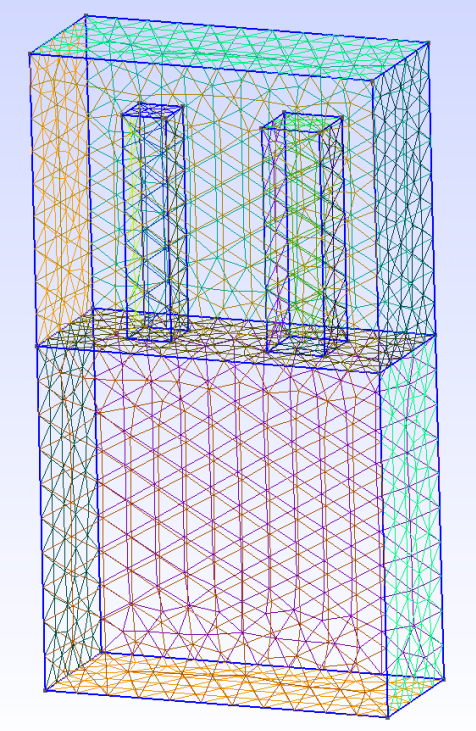

Figure 4.2: The mesh of the setup with 2 pillars, created in Gmsh.

The second requirement was that of the inward pointing electric field components only creating a field inside the objects. Figure 4.4 shows that this is still true in the case of two pillars.

Similarly, the requirement of the outgoing field only existing outside the entire object, but for the different parts being allowed to also exist inside, also still holds, as can be seen in figure 4.5.

Finally, also the requirements for the magnetic field still hold. Figure 4.6 shows the continuity of the magnetic field. The heat maps for the other requirements are similar to the ones of the electric field. They can be found by running the program named “Pillar12.jl” from [9].

4.4. Conclusion

The question was whether the simulations still work when the object consists of two pillars on a substrate covered with an encapsulant instead of one pillar. The solutions to the simulations of two pillars all meet the requirements. This means that they are indeed solutions to the Maxwell equations. Thus, the simulations still work for the object containing two pillars.

4.5. Discussion

All simulations in this chapter were run on a standard laptop, just like in the case of one pillar. However, by adding the second pillar, the total area of the surfaces increased. This meant that with the same variable h, the mesh contained more triangles and therefore the simulation had more unknowns. To be able to still run the simulations with the memory available, h had to be increased, so the accuracy of the simulation decreased. Fortunately, there still does not seem to be a reason to assume the simulation will not work for a finer mesh.

The high amount of memory required by the simulations leads to the question whether there is a way to decrease this amount. The next chapter will discuss two instances of one possible way to do this.

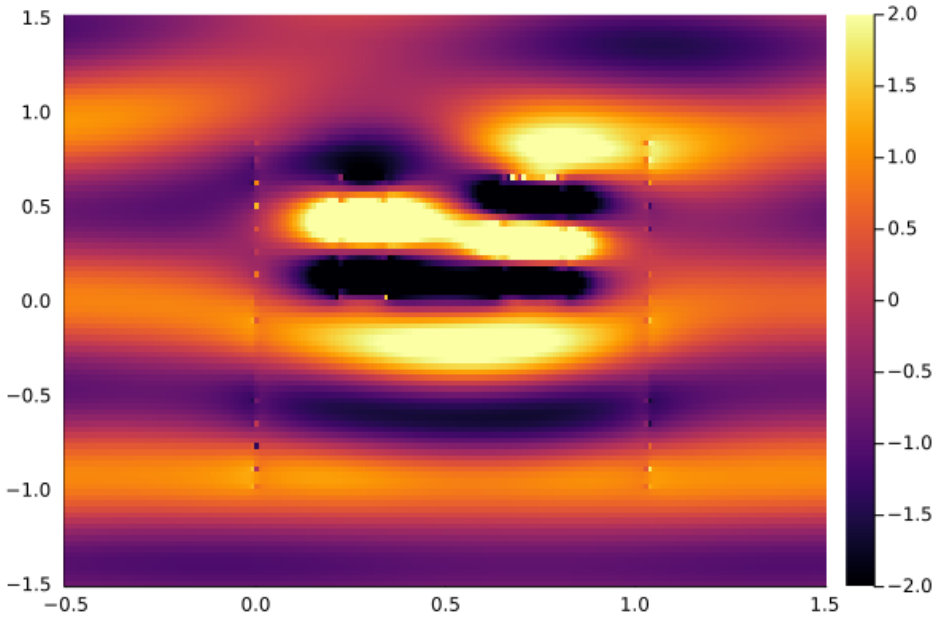

Figure 4.3: Heat map showing the x-component against the z-component of the total electric field of pillars 1 and 2. To be a solution to the Maxwell equations, the map should be continuous when walking from the bottom to the top.

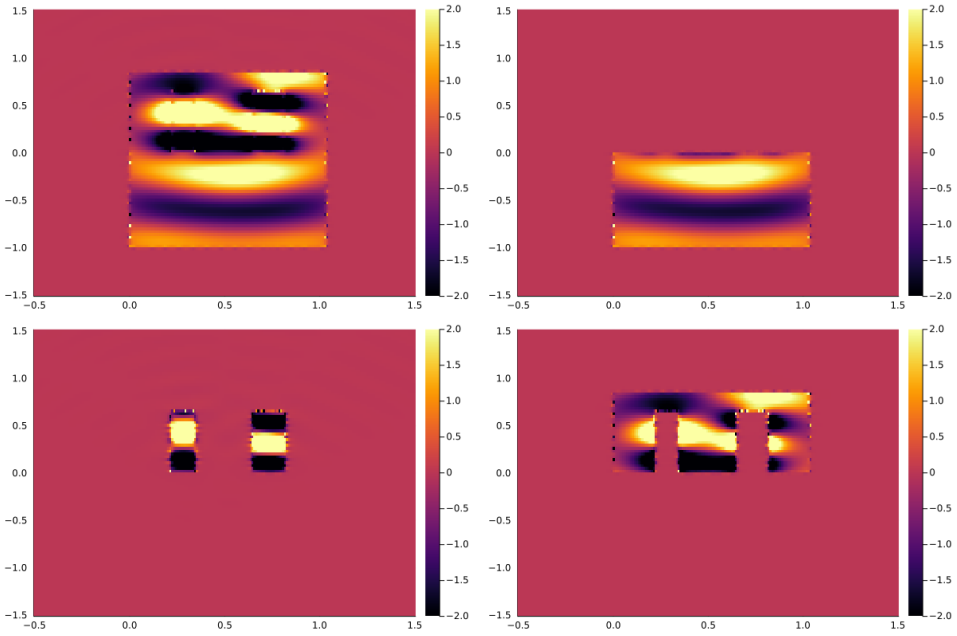

Figure 4.4: The inward pointing electric field components. Top left: The total inward pointing electric field. Top right: the inward pointing electric field component of the substrate. Bottom left: The inward pointing electric field component of pillars 1 and 2. Bottom right: The inward pointing electric field component of the encapsulant. In all four cases, the field meets the requirement of only existing inside the object and being equal to zero outside the object.

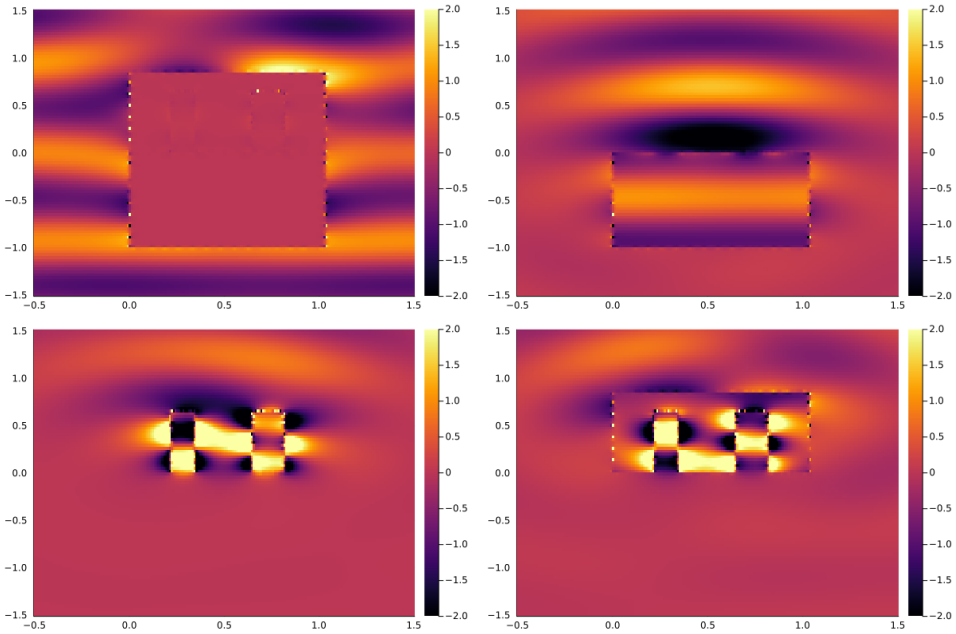

Figure 4.5: The outward pointing electric field components. Top left: the total outward pointing electric field component. Top right: the outward pointing electric field component of the substrate. Bottom left: the outward pointing electric field component of pillars 1 and 2. Bottom right: the outward pointing electric field component of the encapsulant.

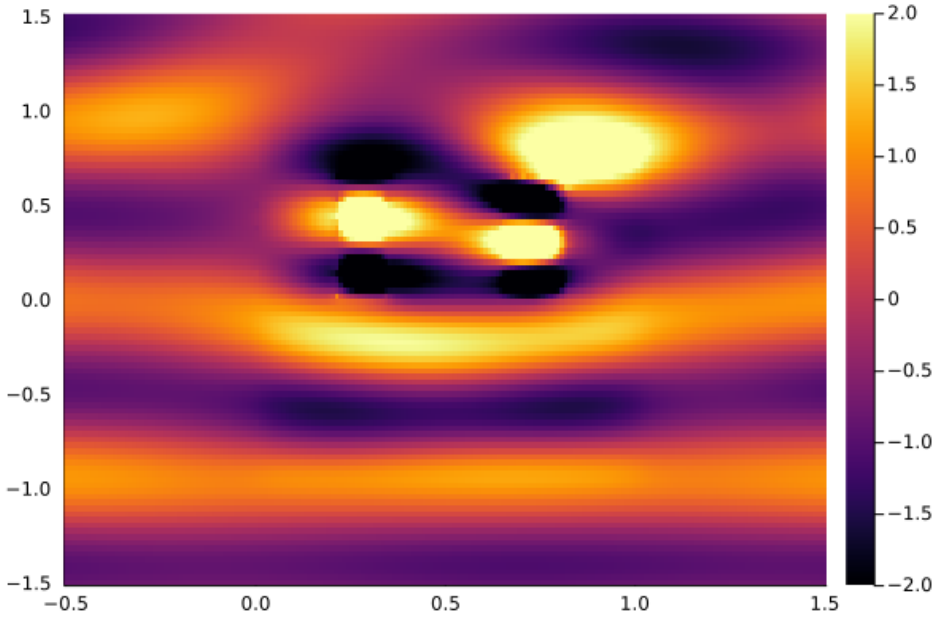

Figure 4.6: Heat map showing the y-component against the z-component of the total magnetic field of pillars 1 and 2. To be a solution to the Maxwell equation, the map should be continuous when walking from left to right.

5

Preconditioned Simulation of Scattering by 1 Pillar

The previous chapters show that the simulation works for one pillar as well as two pillars. As mentioned in chapter 4, the simulation takes up too much memory to be able to simulate all five pillars on my laptop. Therefore, this chapter discusses a possible change to the program that should decrease the amount of memory needed and make the program faster. First, the problem will be explained. Next, it will be explained what method was used to solve the problem. Finally, the results of this method will be discussed.

5.1. Problem definition

As mentioned in the previous chapters, the programs take a long time to run and require a large memory. The simulations run, are relatively simple and the meshes are not very fine yet. However, my laptop cannot run a finer mesh, or a more complicated setup. This gave rise to the question this chapter will answer: ”Is there a way to limit the amount of additional memory needed when complicating the setup further?”. This chapter will look at two instances of one technique that could limit the memory needed. As will be explained is section 5.2.1, this technique aims to decrease the number of iterations needed to find the solution, by changing the matrix before the iterative process starts.

5.2. Method

This section discusses how “preconditioning” might reduce the amount of iterations needed without changing the resulting electromagnetic field. After that, it will explain how the program has to be adjusted to incorporate preconditioning.

5.2.1. Preconditioning

To find the solution of the matrix equation $Ax = b$, the program iterates over possible solutions, until it finds one within a certain range of error. The idea of preconditioning is to multiply both sides of this equation with a matrix P in such a way that the number of iterations needed to solve the new matrix equation is less than the original number of iterations needed, without changing the outcome. An example of a matrix that does this, is A^{-1}, since then the equation becomes $Ix = A^{-1}b$, with I the identity matrix. However, the inverse of A does not always exist. This does give rise to the idea of what we want our matrix P to be. We want P to be close to what would be A^{-1}, if it would exist. This chapter will discuss two matrices, preconditioners, of this type: the Calderón preconditioner and the block-Jacobi preconditioner and give an intuitive idea of why these matrices might work.[3]

For a precise description of how to construct the Calderón preconditioner P and a description of what it looks like, see [1]. The Calderón preconditioner consists of several integral operators, which in turn contain derivatives. It is constructed in such a way that the integrals in the preconditioner and the derivatives in A cancel and the derivatives in the preconditioner and the integrals in A also cancel. This

results in a matrix close to I and therefore P is close to A^{-1}.[3]

The original matrix A consists of several blocks. Instead of finding the inverse of A, the block-Jacobi method takes the inverse of each of the diagonal blocks of A. The block-Jacobi preconditioner J has these inverse blocks on the diagonal and zeroes for all other entries. Intuitively, it probably is not surprising that this matrix is close to A^{-1}[3].

5.2.2. Program Adjustments

We want to be able to compare the number of iterations needed with a preconditioner to the number of iterations needed without a preconditioner. Therefore, the program calculates the solution both with and without a preconditioner and returns both numbers of iterations. This means that the first part of the program remains the same and an extra part containing the preconditioner is added. This means that first the preconditioner matrix is created. In “Pillar1_Calderon_preconditioned.jl” this happens in lines 116-139 and in “Pillar1_Jacobian_preconditioned.jl” this happens in lines 116-135. Both files can be found in [9]. After this, the new matrix equation is created by multiplying both sides of the old equation by the preconditioner matrix. The equation is solved and the program returns the number of iterations needed to solve the original matrix equation and the number of iterations needed to solve the new matrix equation.

An important thing to note is that the number of iterations depends on the number of unknowns. However, if the number of unknowns does not change between two runs, then neither does the number of iterations. The smaller the value of h, the finer the mesh and the higher the number of unknowns. Since this program still calculates the solution in the non-preconditioned way as well, the fineness is still limited by the memory availability of my laptop. Therefore, the choice was made to only get an indication of how well the preconditioners work, instead of looking at their convergence. This means that both programs were run once with $h = 0.075$.

5.3. Results

This section will discuss the results found by running the two programs.

Both programs had the same value for h and therefore the number of iterations needed to solve the original matrix equation was the same for both programs. The number of iterations needed to solve the original matrix equation is equal to 2280. The number of iterations needed to solve the matrix equation after applying the Calderón preconditioner is equal to 580. The number of iterations needed to solve the matrix equation after applying the block-Jacobi preconditioner is equal to 27.

This means that solving the system using the Calderón preconditioner takes about a fourth of the time it takes to solve the system without preconditioner. Solving the system using the block-Jacobi preconditioner is about 85 times faster than solving it without preconditioner. These programs are large and have a long runtime, so this can be the difference between a simulation having a runtime of a week without preconditioner, a runtime of a little under 2 days with the Calderón preconditioner and a runtime of just 2 hours with the block-Jacobi preconditioner.

Furthermore, since the new matrix equation contains a matrix that is close to the identity matrix, it needs less memory to store the new equation, decreasing the amount of memory required to run the program.[3]

5.4. Conclusion

This chapter tried to find a way to decrease the runtime en memory required to run one simulation. It did this by applying two different preconditioners to the matrix equation. It showed that while the Calderón preconditioner results in a significant decrease of the runtime needed, the block-Jacobi preconditioner is significantly better.

5.5. Discussion

To get a more precise result of how much faster the Calderón and block-Jacobi preconditioners are, more runs with different values for h should be done. This way, the convergence can be seen and the true difference can be calculated. This does not mean that the results of this chapter are not true, but they will be more precise after more runs.

6

Conclusion and Future Work

The question asked by Metalenz was whether it is possible to use the multi-trace method to simulate the scattering of an electromagnetic wave by their test-case object. The object consists of five pillars of varying diameter, placed on a substrate and covered by an encapsulant.

To solve this problem, the multi-trace method in combination with the frequency domain PMCHWT equation was used. The idea of the multi-trace method is to put a small layer of background material, in this case air, between any two domains of different materials. The frequency domain PMCHWT equation can then be used to calculate the electromagnetic fields for each domain.

First, the simulation was tested for one and two pillars. It turned out that while the simulation seemed to work, running it cost a large amount of memory and time. All simulations were run on a standard laptop. This meant that there was a limited amount of memory available, preventing the simulations from being more precise and preventing the possibility of simulating a setup with all five pillars. The last part of the research looked at whether using a preconditioner would decrease the amount of time and memory required by the simulation by reducing the amount of iterations needed. It turned out that the Calderón preconditioner would make it approximately four times faster and the block-Jacobi preconditioner would make it approximately 85 times faster.

To conclude, based on the results of this research, it seems likely that the multi-trace method can be used to simulate the scattering of an electromagnetic wave by the test-case object provided by Metalenz. However, since the simulations take up a large amount of memory, it was not possible to run the simulation for the setup with all five pillars. To run that simulation, the block-Jacobi preconditioner can be used, because it significantly reduces the number of iterations needed to solve the matrix equation in the simulation.

There are several ways to continue from this research. The first step would be to implement the block-Jacobi preconditioner with some different values for h, to see how it converges. If it does indeed significantly reduce the iteration count for finer meshes as well, the next step would be to implement the simulation for the setup with all five pillars using the block-Jacobi preconditioner. After that, more complicated designs can be tested, for example placing five of these rows behind each other to form a five by five square of pillars or making all pillars of a different material. However, for these last options a good computer is required, maybe even a supercomputer like the one TU Delft is planning to build, depending on the fineness of the mesh.

Bibliography

[1] Yves Beghein. *Advanced Discretization and Preconditioning Techniques for Electromagnetic Boundary Integral Equations*. PhD thesis, Universiteit Gent, 2016.

[2] X. Claeys, R. Hiptmair, C. Jerez-Hanckes, and S. Pintarelli. Novel multi-trace boundary integral equations for transmission boundary value problems. 2014.

[3] K. Cools. Notes from supervisor. 2021.

[4] Gmsh. Gmsh. `https://gmsh.info/`. Accessed: 01-05-2021.

[5] R. Hiptmair, C. Jerez-Hanckes, JF. Lee, and Z. Peng. Domain decomposition for boundary integral equations via local multi-trace formulations. *Domain Decomposition Methods in Science and Engineering XXI*, 2014.

[6] J.D. Jackson. *Classical Electrodynamics*. Wiley, New York City, New York, 1962.

[7] Jian-Ming Jin. *Theory and Computation of Electromagnetic Fields*. 2010.

[8] Metalenz. Metalenz. `https://www.metalenz.com/`. Accessed: 01-05-2021.

[9] Annerieke Ohm. Github repository. `https://github.com/Anneriekeo/BEP_Multitrace`.